Fluid Flow in Compressible Porous Media: II: Dynamic Behavior

K. Ann-Sofi Jönsson and Bengt T. L. Jönsson
Dept. of Chemical Engineering I, Lund University, S-221 00 Lund, Sweden

This article deals with the dynamic behavior during filtration and wet pressing of compressible porous media. An equation is developed which permits the derivation of the time dependency of porosity and flow at varying locations in a medium subjected to hydraulic pressure and/or mechanical load. Furthermore, a numerical solution that allows the equation to be solved rapidly and with high accuracy on a common PC is presented. The computer program developed in conjunction with this work has been used to illustrate the dynamics of fluid flow in some industrially important applications, such as wet pressing of paper pulp and flow in chromatography columns. The program has also been used to calculate the flow and concentration variations during mechanical impulse loading (that is, a press pulse).

Introduction

The fundamental aspects of flow in porous media have been discussed in a vast number of articles. However, most describe the fluid flow in rigid materials. When fluid flow in compressible media is described the difficulty lies in that mechanical loads, as well as drag forces, deform the solid matrix. This mechanical and hydraulic pressure-induced compression of the matrix results in an increased resistance to liquid flow due to a decrease in the interstitial space.

A theoretical flow model relating pressure and steady-state fluid flow in a compressible porous media was derived in a previous article (Jönsson and Jönsson, 1992). In this article a flow equation is presented which allows the derivation of the time dependency of porosity and flow at varying locations in the medium. The presented equation allows the dynamics of media subjected to a compressive stress induced by hydraulic pressure and/or a mechanical load to be studied.

Knowledge about the dynamic flow conditions of porous media is of the utmost importance in many industrial applications; papermaking being probably the one of greatest economic importance. Increasing the efficiency of the press section of paper machines is an attractive route to achieving energy savings. Hence, great efforts have been made to develop tools for papermakers to predict and control the water removal during wet pressing of paper webs (Nilsson and Larsson, 1968; Westra, 1975; Jewett et al., 1982; Caulfield et al., 1982; Ceckler et al., 1982; Vincent et al., 1988; Burns et al., 1990; Roux and Vincent, 1991). A comprehensive review of articles treating the dynamics of water flow during wet pressing has recently been published by El-Hosseiny (1991).

The use of the numerical program, developed in conjunction with this work, is illustrated by following flow and porosity variations during filtration and during wet pressing of compressible porous media. The influence of pressure and compressibility on porosity and the dynamic behavior of a medium during a press pulse are also discussed.

Dynamic Fluid Flow Equation

In a previous article (Jönsson and Jönsson, 1992) an expression describing fluid flow through compressible porous media under stationary conditions was derived. The description of the dynamic behavior derived in this paper is based on the same basic assumptions:

- The total volume of the porous medium can be divided into the volume of solid material, V_s, the volume of adsorbed water, V_a, and the void volume, V_v. The volume that the solid material and adsorbed water occupy, V_{sa}, is regarded as an incompressible part of the medium and thus, deformation of the medium affects only the void volume, V_v.
- There is no mixing of solid material between different layers in the solid matrix. A layer may be compressed, or

Correspondence concerning this article should be addressed to K. A.-S. Jönsson.
Address of B. T. L. Jönsson: Physical Chemistry I, Lund University, P.O. Box 124, S-221 00 Lund.

expanded, but no transport of solid material out from, or into, the layer is allowed.

The second assumption, of there being no interlayer transport of material, makes it practicable to introduce a new coordinate system which is denoted the y-coordinate system. This system is assumed to be moving with the solid particles so that the volume of the solid material and adsorbed water, ΔV_{sa}, in a volume element of thickness Δy is unchanged during compression. The amount of solid, Δm_s, is the same in each element Δy:

$$\Delta m_s = WA\Delta y \tag{1}$$

where W is the basis weight and A is the cross-sectional area of the medium.

The normal z- and the y-coordinate systems are related by the correlation (Jönsson and Jönsson, 1992):

$$\frac{dz}{dy} = W\nu_{sa}(1+X) \tag{2}$$

where ν_{sa} is the specific obstruction volume of the medium:

$$\nu_{sa} = \frac{V_{sa}}{m_s} \tag{3}$$

and X is the void ratio defined as:

$$X = \frac{V_v}{V_{sa}} \tag{4}$$

The change in the volume of an element with thickness Δy is:

$$\frac{d\Delta V}{dt} = \frac{d}{dt}\left[\Delta V_{sa}(1+X)\right] = \Delta[m_s\nu_{sa}(1+X)] = \Delta m_s\nu_{sa}\frac{dX}{dt} \tag{5}$$

as the time derivative of the mass of solid material, $d\Delta m_s/dt$, is zero in the y-coordinate system as stated earlier.

The time derivative of this volume of water may also be expressed as the difference in the flow of water into, $J(y+\Delta y)$, and out of, $J(y)$, the volume element, see Figure 1.

$$\frac{d\Delta V}{dt} = A[J(y+\Delta y) - J(y)] = A\Delta y\frac{dJ}{dy} \tag{6}$$

Combination of Eqs. 1, 5 and 6 yields:

$$\frac{dX}{dt} = \frac{1}{W\nu_{sa}}\frac{dJ}{dy} \tag{7}$$

The correlation between fluid flow and pressure drop across a medium may be derived from Darcy's law and expressed in the general form (Jönsson and Jönsson, 1992):

$$J(y) = \frac{\nu_{sa}}{\mu W S_s^2}K(X)\frac{dP_h}{dy} \tag{8}$$

where μ is the viscosity of the fluid, S_s is the surface exposed to the fluid per unit mass of solid material, $K(X)$ is the permeability, that is, the resistance to flow of the matrix, and P_h is the hydraulic pressure which gives rise to the fluid flow.

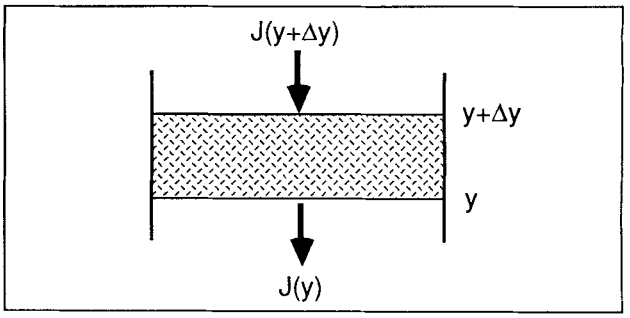

Figure 1. Flow through a thin layer Δy of a compressible porous medium.

The variation of void ratio with time may be derived from Eqs. 7 and 8 as:

$$\frac{dX}{dt} = \frac{1}{\mu W^2 S_s^2}\frac{d}{dy}\left[K(X)\frac{dP_h}{dy}\right] \tag{9}$$

The hydraulic pressure is, however, only one of two pressure components which together constitute the total applied pressure, P_{tot}:

$$P_{\text{tot}} = P_h + P_m \tag{10}$$

The mechanical pressure, or the mechanical stress in the bed, P_m, deforms the bed until an equilibrium position is reached. In this article it is assumed that the matrix is always in mechanical equilibrium. The variation of the specific void volume with time in a bed element is thus governed by the permeability of the medium. We may then apply the general statement that the equilibrium specific void volume in an element depends on the applied mechanical pressure and vice versa.

Insertion of the relation between the hydraulic and the mechanical pressure:

$$\frac{dP_h}{dy} = \frac{d(P_{\text{tot}} - P_m)}{dy} = -\frac{dP_m}{dy} \tag{11}$$

into Eq. 9 gives the result:

$$\frac{dX}{dt} = -\frac{1}{\mu W^2 S_s^2}\frac{d}{dy}\left[K(X)\frac{dP_m}{dy}\right] \tag{12}$$

Equation 12, together with expressions for the compressibility and permeability of the medium, permits the derivation of the time dependency of the void ratio at varying locations in the medium. Any optional permeability function $K(X)$, and compressibility function $P_m(X)$ may be used. In the following examples the permeability expression for flow perpendicular to cylinders, Eq. 30, and the compressibility Eqs. 24 and 26 from (Jönsson and Jönsson, 1992) have been used.

Numerical Solution

The numerical solution is based on a finite-element method.

In this the bed is divided into a number of small elements. The variation of the void ratio during a short time interval is calculated in each element by Eq. 12:

$$-\Delta X(n, t_o)\mu W^2 S_s^2 = \int_{t_o}^{t_o+\Delta t} F(n, t)dt \tag{13}$$

where

$$\Delta X(n, t_o) = X(n, t_o+\Delta t) - X(n, t_o) \tag{14}$$

and

$$F(n, t) = \frac{d}{dy}\left[K(n, t)\frac{dP_m(n, t)}{dy}\right] = \frac{dK(n, t)}{dy}\frac{dP_m(n, t)}{dy} + K(n, t)\frac{d^2P_m(n, t)}{dy^2} \tag{15}$$

For small Δt the integral may be approximated by the trapezoid rule and Eq. 13 may then be written:

$$-\Delta X(n, t_o)\frac{2\mu W^2 S_s^2}{\Delta t} = F(n, t_o) + F(n, t_o+\Delta t) \tag{16}$$

The three derivatives in Eq. 15 are then replaced by differences:

$$\frac{dP_m(n, t)}{dy} \approx \frac{P_m(n+1, t) - P_m(n-1, t)}{2\Delta y} \tag{17a}$$

$$\frac{dK(n, t)}{dy} \approx \frac{K(n+1, t) - K(n-1, t)}{2\Delta y} \tag{17b}$$

and

$$\frac{d^2P_m(n, t)}{dy^2} \approx \frac{P_m(n+1, t) - 2P_m(n, t) + P_m(n-1, t)}{\Delta y^2} \tag{17c}$$

A further simplification is to assume only small changes in $P_m(n, t)$ and $K(n, t)$ during the small time interval from t_o to $t_o + \Delta t$ and to linearize the two functions in X:

$$P_m[X(n, t_o+\Delta t)] \approx P_m[X(n, t_o)] + P_m'[X(n, t_o)]\Delta X(n, t_o) \tag{18a}$$

and

$$K[X(n, t_o+\Delta t)] \approx K[X(n, t_o)] + K'[X(n, t_o)]\Delta X(n, t_o) \tag{18b}$$

The right side of Eq. 16 may then be written as:

$$F(n, t_o) + F(n, t_o+\Delta t) \approx \frac{[A + B\Delta X(n-1) + C\Delta X(n) + D\Delta X(n+1)]}{4(\Delta y)^2} \tag{19}$$

where

$$A = 2\{[K(n+1) - K(n-1)][P_m(n+1) - P_m(n-1)] + 4K(n)[P_m(n+1) - 2P_m(n) + P_m(n-1)]\}_{t_o} \tag{20a}$$

$$B = -\{K'(n-1)[P_m(n+1) - P_m(n-1)] + P_m'(n-1)[K(n+1) - K(n-1) - 4K(n)]\}_{t_o} \tag{20b}$$

$$C = \{4K'(n)[P_m(n+1) - 2P_m(n+1) + P_m(n-1)] - P_m'(n)K(n)\}_{t_o} \tag{20c}$$

$$D = \{K'(n+1)[P_m(n+1) - P_m(n-1)] + P_m'(n+1)[K(n+1) - K(n-1) + 4K(n)]\}_{t_o} \tag{20d}$$

For $0 < n < N$ Eq. 16 may now be written as:

$$B\Delta X(n-1) + \left[C + \frac{2\mu}{\Delta t}(2WS_s\Delta y)^2\right]\Delta X(n) + D\Delta X(n+1) = -A \tag{21}$$

In order to solve Eq. 21 the void ratio, or the derivative of the void ratio, at the bottom of the bed, $n = 0$, and at the top of the bed, $n = N$, must be known as a function of time.

The void ratio in the bottom layer may be obtained from Eq. 24 in (Jönsson and Jönsson, 1992) since the mechanical pressure on this layer is the same as the sum of the applied mechanical and hydraulic pressures.

If fluid is flowing into or out of the bed through the top layer the void ratio at this point is calculated by inserting the mechanical pressure applied on the bed in Eq. 24 in Jönsson and Jönsson (1992).

If, on the other hand, there is no fluid flow through the top layer, the derivative of the void ratio will be zero at this point:

$$dX(N, t)/dy = 0 \tag{22a}$$

or Eq. 21 may be used with:

$$X(N+1) = X(N-1) \tag{22b}$$

The functions $K(X)$ and $P_m(X)$ in Eq. 21 are substituted by appropriate empirical or theoretical expressions for the permeability and compressibility of the medium.

Apart from the boundary conditions discussed above, we need to know the highest mechanical pressure the medium has been subjected to and starting-point values for the void ratio at all points in the system. The simplest example of starting-point values is when the void ratio is constant throughout the whole bed. This is the starting point we have used in all the examples in this article, but the calculations are by no means restricted to this simple void ratio distribution.

Application of the Model

The influence of drag forces exerted by a flowing liquid, and the influence of an applied mechanical load on fluid flow and pore space in a compressible porous material may be evaluated by the model presented in this article. The following applications, each treated in detail below, illustrate the use of the model:

- A liquid is forced through a compressible porous medium.

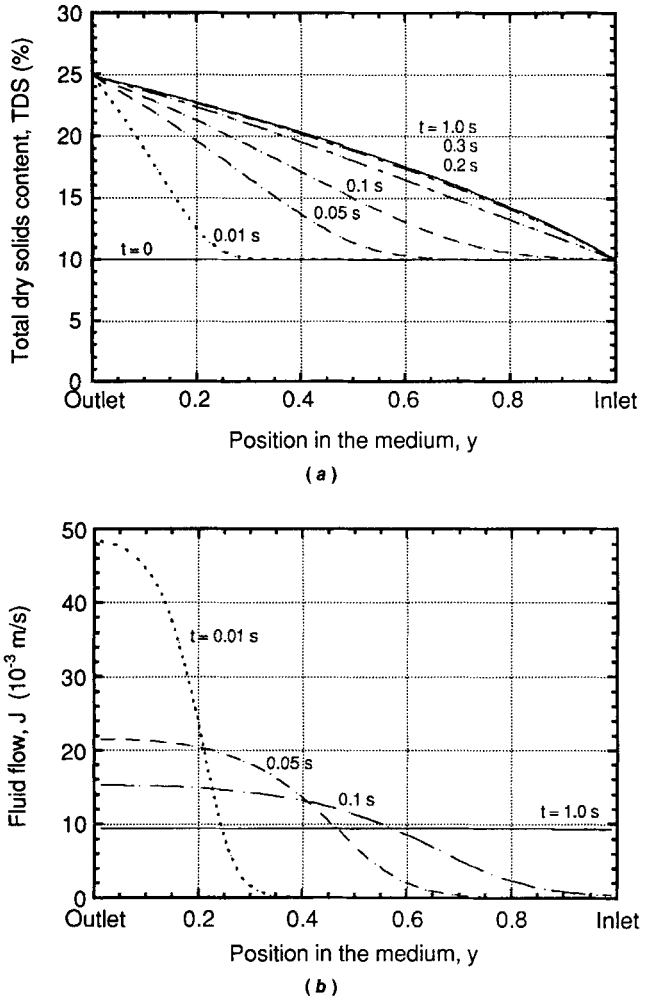

Figure 2. Development of (a) solids content and (b) flow gradients in a compressible porous medium.

The applied hydraulic pressure of the fluid was 100 kPa. The parameters in Eq. 12 were assigned the following values: $\nu_{su} = 0.92 \times 10^{-3}$ m^3/kg; $\mu = 0.9 \times 10^{-3}$ Pa·s; $S_s = 2{,}000$ m^2/kg; $W = 1$ kg/m^2; $N = 0.45$. A constant applied mechanical pressure of 8.13 kPa, corresponding to an initial porosity of 0.90 (= solids content of 10%) was also used. The fluid flow through an incompressible material during corresponding operating conditions is 19×10^{-3} m/s.

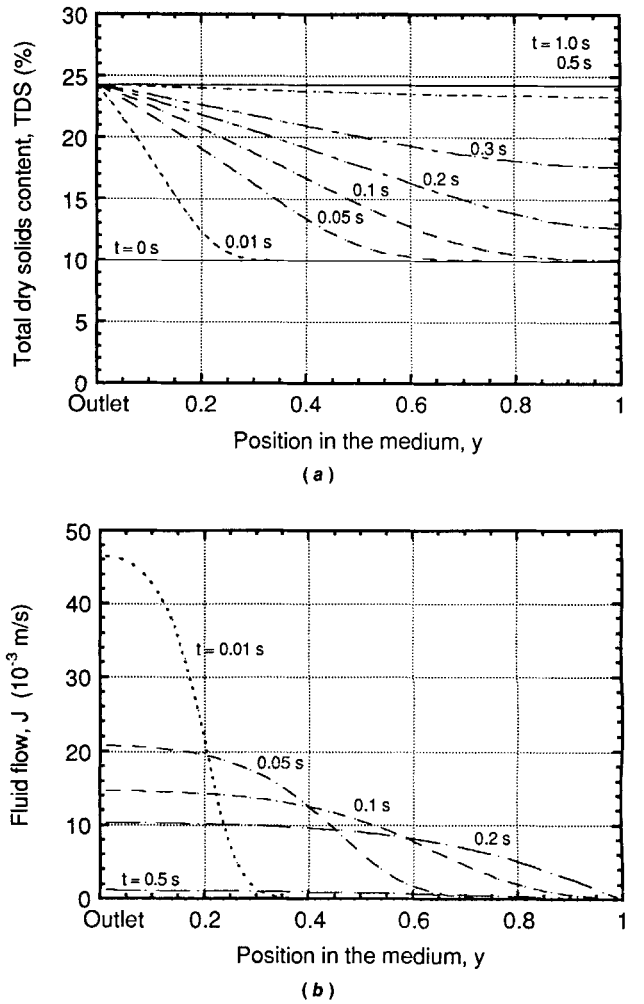

Figure 3. Development of (a) solids content and (b) flow gradients in a compressible porous medium during one-sided expression of water.

The applied mechanical pressure was 100 kPa. No hydraulic pressure was applied. The values of the compressibility and permeability parameters are the same as in Figure 2.

The only external, applied pressure is the hydraulic pressure of the liquid. Example: filtration in chromatography columns and washing of fiber beds.

- Expression of water from a medium. A mechanical load is the only external, applied pressure. Example: wet pressing of paper pulp.
- Hydraulic and mechanical pressure are applied simultaneously. Example: washing of fiber beds in a wash press.

Fluid flow through a compressible porous medium

The influence of the physical properties of compressible porous media on the *steady-state fluid* flow was analyzed in a previous article (Jönsson and Jönsson, 1992). The *dynamic* behavior of a bed subjected to a hydraulic pressure exerted by a flowing liquid is shown in Figure 2, where the solids content and fluid flow at various locations in the bed at different times are given. As shown in Figures 2a and 2b, steady-state conditions are reached relatively rapidly.

There is a considerable difference between the behavior of a medium subjected to a continuous transport of water, as in Figure 2, and a medium from which water is expressed.

Expression of a liquid

During filtration there is a continuous transport of water through the porous medium, whereas during expression water transport stops when the solids content corresponding to the applied pressure is reached. In Figure 3 the solids content and fluid flow at various locations in a compressible porous media at different times during expression of water are shown.

As shown in Figure 3a, the layers nearest the point of water removal compact first and reach the final steady-state solids content in a very short time. The compaction progressively extends through the medium with the layers next to the nonpermeable surface (that is, at $y = 1$) being compacted at a slower rate than those further away. At the nonpermeable

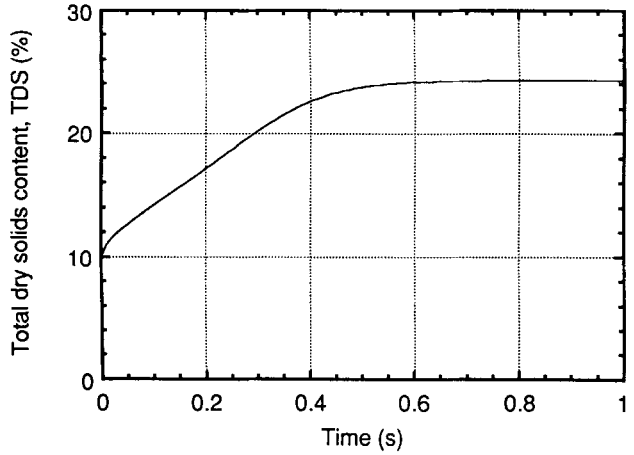

Figure 4. Increase of average solids content with time in a fibrous material subjected to a mechanical pressure of 100 kPa.

Values of the parameters in Eq. 12 are the same as in Figure 3.

surface the solids content corresponding to the applied pressure is not reached until water removal has stopped and the whole of the pressure is borne by the solids.

At the beginning of the expression water flow is restricted to the bottom layers of the bed, as shown in Figure 3b. When water transport through the top layers of the bed begins the bottom layers of the bed are already compressed and the velocity of the flowing liquid progressively decreases. However, usually it is not the concentration at specific locations, but the average solids content of the whole sample that is of interest during expression operations. In Figure 4 the increase in the average solids content with time for the bed illustrated in Figure 3 is shown.

Influence of pressure and compressibility on the solids content

The final solids content of a compressible porous medium

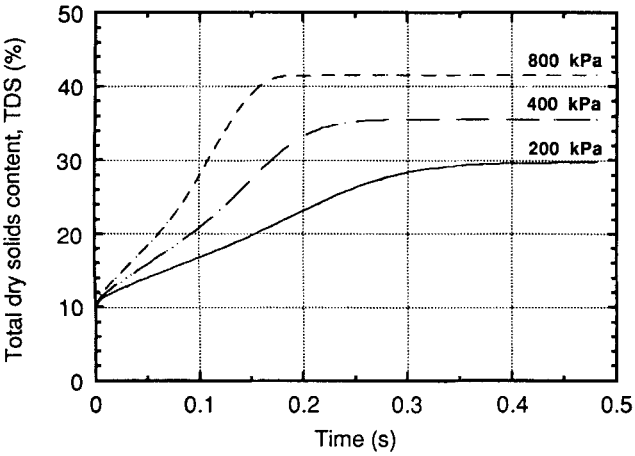

Figure 5. Influence of applied pressure on solids content of a fibrous material.

The parameters in Eq. 12 were assigned the following values: $\nu_{sa} = 0.92 \times 10^{-3}$ m^3/kg; $\mu = 0.9 \times 10^{-3}$ Pa·s, $S_s = 2{,}000$ m^2/kg; $W = 1$ kg/m^2; $N = 0.45$; $P_h = 0$. The initial solids content was 10%.

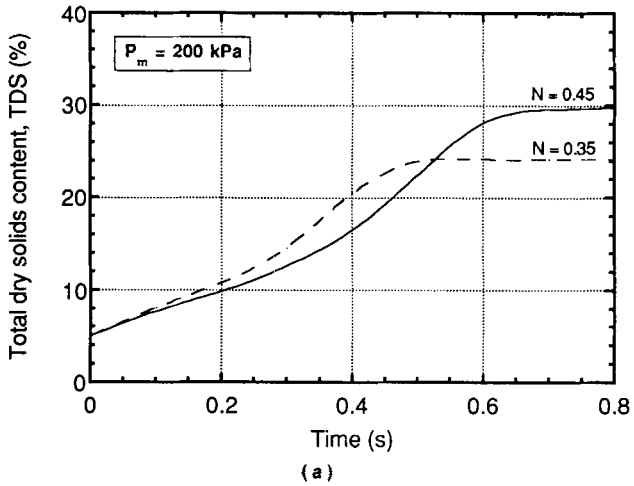

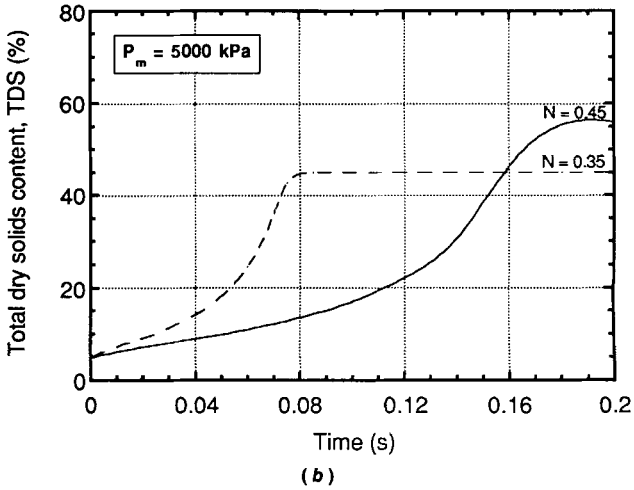

Figure 6. Increase in solids content with time for fibrous materials of different mechanical strength at an applied mechanical pressure of (a) 200 kPa and (b) 5,000 kPa.

The parameters in Eq. 12 were assigned the following values: $\nu_{sa} = 0.92 \times 10^{-3}$ m^3/kg; $\mu = 0.9 \times 10^{-3}$ Pa·s; $S_s = 2{,}000$ m^2/kg; $W = 1$ kg/m^2; $P_h = 0$. The initial solids content was 5%.

is governed by two factors: the magnitude of the applied pressure and the mechanical strength, or compressibility, of the medium.

Obviously, the solids content increases with increasing applied pressure but, as shown in Figure 5, the steady-state solids content is also reached more rapidly at a higher applied pressure.

The parameter N is a measure of the compressibility of a porous medium. The higher the value of N, the more compressible the medium. However, not only the solids content, but also the time needed to reach the final equilibrium concentration increases with increasing N. The increase in solids content with time for two materials of different mechanical strength is shown in Figure 6.

The stiffest material (the material with $N = 0.35$ in Figure 6) has a higher porosity, and thus a better permeability, and therefore reaches its steady-state value first. As water from the top layers has to be transported through to the bottom

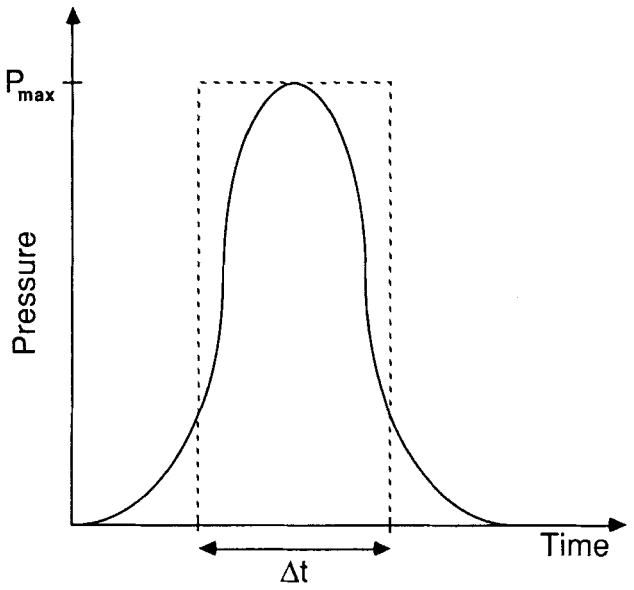

Figure 7. Rectangular approximation of pressure distribution curve.

layers of the bed, which instantaneously reach their final porosity, it is natural that this process takes longer for a more compressible material.

In Figure 6 it can also be seen that the difference between materials of different mechanical strength is more pronounced at higher pressures.

Press pulse

Many applications include a mechanical impulse loading; the press section of paper machines being probably the most important industrial application. The characteristics of the press pulse to which the paper web is subjected in the press nip of a paper machine depends on nip geometry and line speed, that is, factors specific for each individual paper machine. Any press pulse can be included in the presented model, but in order to give a more generalized description of the influence of an impulse loading the pressure pulse in this presentation is approximated by a rectangular pulse, as shown in Figure 7.

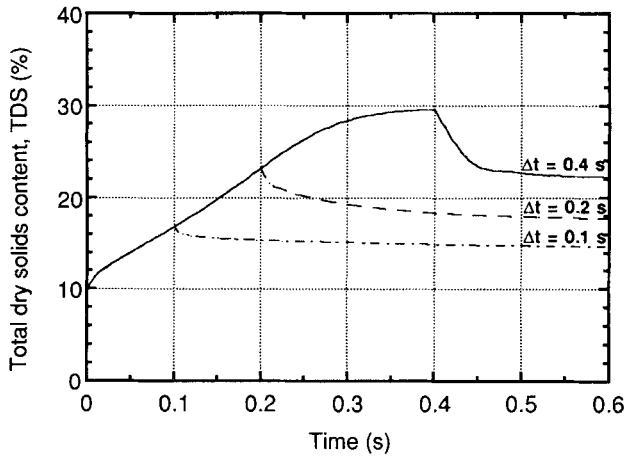

Figure 8. Solids content of a fibrous material subjected to a press pulse of varying duration, 0.1, 0.2 and 0.4 s.

The parameters in Eq. 12 were assigned the following values: $\nu_{so}=0.92\times10^{-3}$ m^3/kg; $\mu=0.9\times10^{-3}$ Pa·s; $S_s=2{,}000$ m^2/kg; $W=1$ kg/m^2; $N=0.45$; $P_h=0$; $P_m=200$ kPa. The initial solids content was 10%.

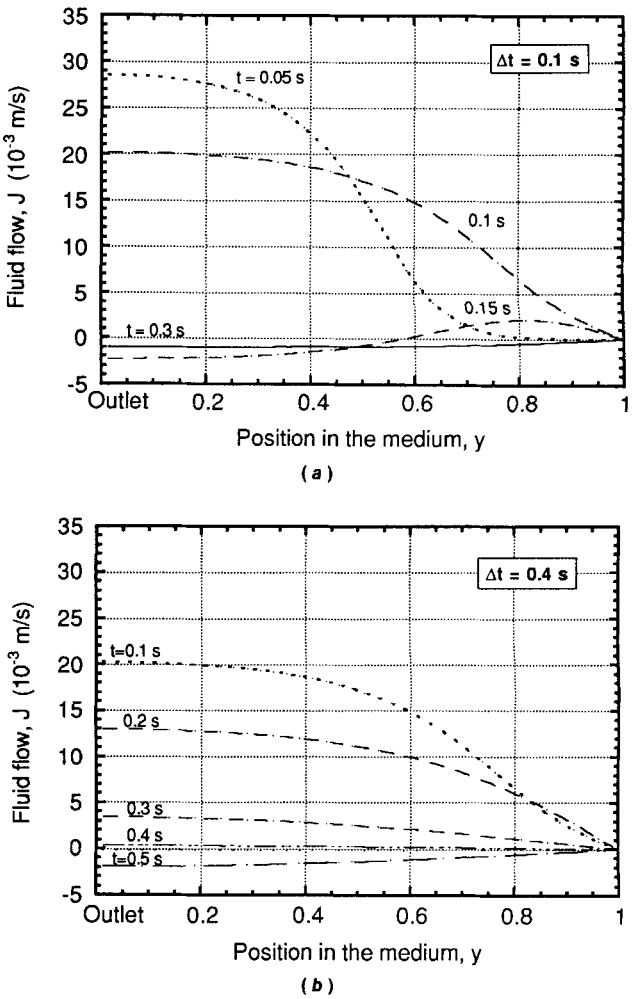

Figure 9. Solids content gradients in a sample subjected to a mechanical pressure of 200 kPa during (a) 0.1 s and (b) 0.4 s.

Values of the parameters in Eq. 12 are the same as in Figure 8.

The average solids content in the web with varying durations of the press pulse has been calculated. As shown in Figure 8 the final solids content is lower than the solids content corresponding to the applied maximum pressure. This is due to the expansion of the paper web when the compressive stress is removed. The relaxation of paper pulp is a well-known phenomenon (Wrist, 1964; Nilsson and Larsson, 1968; Andersson and Gärdh, 1970; Robertson and Haglund, 1974; Jaavidaan et al., 1988). Compressibility relationships useful in describing this phenomenon have been discussed earlier (Jönsson and Jönsson, 1992).

Somewhat surprisingly, the difference between the highest solids content achieved and the final solids content increases with the duration of the press pulse. However, the flow gradients, shown in Figure 9, for the short and the long press pulse in Figure 8, illustrate the explanation of this observation.

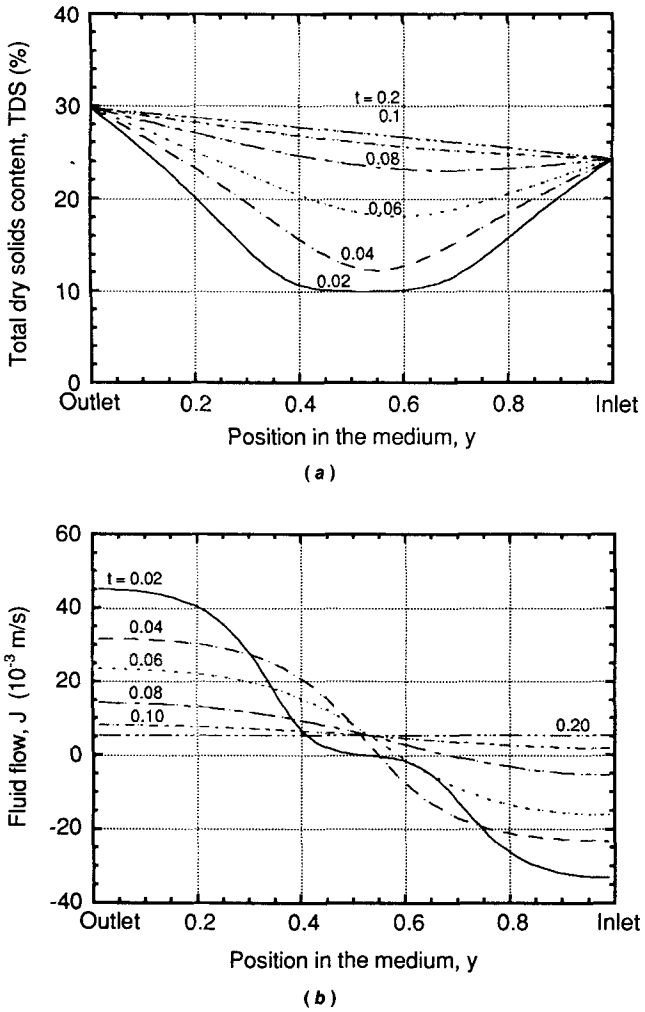

Figure 10. Development of (a) solids content and (b) flow gradients in a compressible porous medium.

The total applied pressure was 200 kPa consisting of a mechanical load of 100 kPa and an applied hydraulic pressure of 100 kPa. The parameters in Eq. 12 were assigned the following values: $\nu_{sa} = 0.92 \times 10^{-3}$ m^3/kg; $\mu = 0.9 \times 10^{-3}$ Pa·s; $S_s = 2{,}000$ m^2/kg; $W = 1$ kg/m^2; $N = 0.45$. The initial porosity was 0.90 (= solids content of 10%).

The flow gradient at $t = 0.15$ s in Figure 9a shows the transport of water in the bed when the mechanical load is removed. When the bottom layers expand some of the water is sucked back (as illustrated by the negative flow gradient at the outlet part of the bed). However, in the inlet part of the bed the flow gradient is positive, which indicates that the outlet part of the bed also sucks water from this part of the sample. The conclusion is that during the expansion following a short press pulse, mainly water *within* the sample is redistributed.

During a long press pulse, most of the water has been expressed (and a higher solids content thus reached). When the mechanical load is removed expressed water is reabsorbed in the sample, as indicated by the negative flow gradient throughout the whole sample at $t = 0.5$ s in Figure 9b.

Simultaneous application of hydraulic and mechanical pressure

In the above examples the expression of water was restricted to one side of the sample. Steady-state conditions are, of course, reached much more quickly when water can leave both at the bottom and the top of the sample. The development of the concentration gradient in a fibrous material during double-sided expression is shown in Figure 10a.

In the example shown in Figure 10 an equally large hydraulic pressure is applied simultaneously with the mechanical load. As demonstrated in Figure 10b the fluid flow gradient is initially negative in the inlet part of the bed, and hence fluid is initially forced in the opposite flow direction.

Conclusion

In this paper an equation is presented which permits the derivation of the time dependency of porosity at various locations in a compressible porous medium subjected to hydraulic pressure and/or a mechanical load. A numerical solution of the flow equation based on a finite-element method is presented. This numerical solution allows the flow equation to be solved quickly (in about one minute) on a (for this type of problem) quite small computer. The examples presented in this paper have been produced on a Macintosh II.

Complex applications, such as press pulses and simultaneously applied external hydraulic and mechanical pressures may also be simulated with this computer program, as illustrated in the article. However, one flow situation that is not encountered in the presented dynamic flow model is the blocking of flow paths by particles and colloids transported with the fluid. The dynamic behavior of this type of medium is characterized by an initial, relatively rapid change in porosity followed by a slow, gradual decrease of flow. The initial change in porosity and flow is described by the presented model, whereas the gradual flow decline is not treated here. The increased resistance to flow due to blocking by fines and colloids is often the factor which controls water removal. This influence may, however, be effectively reduced by the addition of different types of retention aids and in this case the dynamic flow behavior predicted by the presented flow equation agrees rather well with experimental results.

Even though the theoretical flow model presented in this article does not take into account all the complex phenomena which may be encountered during filtration and wet pressing of different types of media, it is our hope that the broadened insight into the flow mechanisms of compressible porous media obtained with the model will foster the development of filtration and dewatering equipment. Areas where the computer program may be useful are in the design of chromatography columns, press sections in paper machines, press felt configuration, and dewatering and washing equipment.

Acknowledgment

This work was financed by the Swedish Board of Technical Development.

Notation

A = cross-sectional area
J = fluid flow per cross-sectional area
K = permeability
m_s = amount of solids
n = number of individual element
N = number of elements into which the medium is divided

N = material-specific compressibility parameter
P_h = hydraulic pressure of the fluid
P_m = mechanical stress exerted on the medium
P_{tot} = total pressure
S_s = surface exposed to the fluid per unit mass of solids
t = time
V_a = volume of adsorbed water
V_s = volume of solid material
V_{sa} = volume of solid material and adsorbed water
V_v = void volume
W = amount of solid component per unit area
X = void ratio
y = length coordinate in an imaginary coordinate system
z = length coordinate in a normal coordinate system

Greek letters

μ = fluid viscosity
v_{sa} = specific obstruction volume

Literature Cited

Andersson, N., and H. Gärdh, "The Compression and Recovery of a Paper Web in a Felted Press," *Sv. Papperstidn.*, **73**(13-14), 425 (1970).

Burns, J. R., T. E. Conners, and J. D. Lindsay, "Dynamic Measurement of Density Gradient Development During Wet Pressing," *Tappi*, **73**(4), 107 (1990).

Caulfield, D. F., T. L. Young, and T. H. Wegner, "The Role of Web Properties in Water Removal by Wet Pressing," *Tappi*, **65**(2), 65 (1982).

Ceckler, W. H., E. V. Thompson, E. R. Ellis, K. B. Jewett, J. F. Hoering, and J. T. Thorne, "The University of Maine Wet Pressing Project and the Application of the Results to Optimization of Press Performance," *Proc. Tappi Eng. Conf., Techn. Assoc. Pulp Paper Ind.*, **1**, 141 (1982).

El-Hosseiny, F., "Mathematical Modeling of Wet Pressing of Paper. A Review of the Literature," *Nordic Pulp and Paper Research J.*, **6**(1), 30 (1991).

Jaavidaan, Y., W. H. Ceckler, and E. V. Thompson, "Rewetting in the Expansion Side of Press Nips," *Tappi*, **71**(3), 151 (1988).

Jewett, K. B., W. H. Ceckler, L. H. Busker, and A. Co, "Computer Model of a Transversal Flow Press Nip," *AIChE Symposium Series*, **76**(200), 59 (1980).

Jönsson, A.-S., and B. Jönsson, "Fluid Flow in Compressible Porous Materials: I: Steady-State Conditions," *AIChE J.*, **38**(9), 1340 (1992).

Nilsson, P., and K. O. Larsson, "Paper Web Performance in a Press Nip," *Pulp Paper Mag. Can.*, **69**, T438 (1968).

Robertson, G., and L. Haglund, "Local Thickness Reduction in a Calendar Nip," *Sv. Papperstidn.*, **77**(14), 521 (1974).

Roux, J. C., and J. P. Vincent, "A Proposed Model in the Analysis of Wet Pressing," *Tappi*, **74**(2), 189 (1991).

Westra, H. A., "A New Contribution to Press Nip Analysis," *Paper Techn. Ind.*, **16**(3), 165 (1975).

Vincent, J. P., B. Lebeau, and J. C. Roux, "A Simulation Tool for the Press Section of the PM," *Paper Techn. Ind.*, **29**(5), 236 (1988).

Wrist, P. E., "The Present State of our Knowledge of the Fundamentals of Wet Pressing," *Pulp Paper Mag. Can.*, **65**, T284 (1964).

Manuscript received Oct. 7, 1991, and revision received Apr. 15, 1992.